J Solid State Electrochem (2010) 14:2293–2305
DOI 10.1007/s10008-010-1064-2

ORIGINAL PAPER

Effect of polyacrylic acid on the corrosion behaviour of aluminium in sulphuric acid solution

Saviour A. Umoren · Ying Li · Fuhui H. Wang

Received: 16 December 2009 / Revised: 26 February 2010 / Accepted: 29 March 2010 / Published online: 23 April 2010

Abstract Electrochemical techniques using both ac and dc as well as surface analyses approach were used to investigate the corrosion inhibition characteristics of polyacrylic acid (PAA) for pure cast aluminium in 0.5 M H_2SO_4 at 30±1 °C. The effect of iodide ion additives was also studied. The results obtained indicate that PAA inhibited the corrosion of pure cast aluminium in the acid medium by adsorption onto the metal surface following Frumkin adsorption isotherm model. Inhibition efficiency increases with an increase in PAA concentration and synergistically enhanced by the addition of iodide ions. A mixed inhibition mechanism is proposed for the inhibitive effects of PAA as revealed by potentiodynamic polarisation technique. Synergism parameter evaluated was found to be greater than unity, indicating that the enhanced inhibition efficiency of PAA on addition of iodide ions was synergistic in nature. Fourier transform infrared analyses revealed that the synergistic effect of iodide ions and PAA is due to co-adsorption of iodide ions and PAA molecules which is cooperative in nature.

Keywords Polyacrylic acid · Aluminium · Synergism · Iodide ion · Adsorption · Acid corrosion

S. A. Umoren · Y. Li (✉) · F. H. Wang
State Key Laboratory for Corrosion and Protection,
Institute of Metal Research, Chinese Academy of Sciences,
62 Wencui Road,
Shenyang 110016, People's Republic of China
e-mail: liying@imr.ac.cn

S. A. Umoren
Department of Chemistry, Faculty of Science, University of Uyo,
P.M.B 1017 Uyo, Nigeria

Introduction

Studies on the corrosion behaviour of aluminium and its alloys have been a hot topic of research in recent times as revealed by the vast number of literature output. This is because aluminium and its alloys are materials of choice in many industrial applications such as automobiles, aviation, electronic devices and building, to mention but a few [1]. Apart from the low density, attractive appearance and excellent thermal and electrical conductivity which convey this position of prime importance, aluminium has relatively good corrosion resistance due to the formation of a compact, adherent passive oxide film on its surface when exposed to air or aqueous solution. However, the protective film is amphoteric and dissolved when Al is exposed to strong acids and alkalis, making aluminium and its alloy prone to corrosion and attendant substantial loss. The best method to protect Al deployed in such service environments is to add corrosion inhibitors.

The influence of several organic compounds containing polar functions such as nitrogen, oxygen, phosphorous or sulphur on the corrosion inhibition behaviour of Al in acid solutions has been documented [1–10]. The effect of any particular organic compound on the corrosion behaviour of metals depends on the type of metal and its interaction with the surface of the corroding metal. The inhibiting effect of organic compounds has been attributed to the adsorption of the compound on the surface of the metal. The adsorption affects the electrochemical behaviour involved in the corrosion processes and is dependent on the chemical structure of the organic compound, the nature and surface charge of the metal, the distribution of the charge in the molecule and the type of aggressive media.

The use of polymers as corrosion inhibitors has attracted considerable attention recently because: (1) they have low

cost and are stable to metallic materials in acid media, (2) possession of multiple adsorption sites and (3) through their functional groups, they form complexes with metal ions, and on the metal surface, these complexes occupy a large area, thereby blanketing the surface and protecting the metal from corrosive agents present in the solution [11–13]. The inhibitive power of these polymers is related structurally to the cyclic rings, heteroatom (oxygen and nitrogen) that are regarded as centres of adsorption. Some polymers have been reported to inhibit the corrosion of Al in various media [14–17]. Polyacrylic acid (PAA) has been reported to inhibit the corrosion of cadmium in HCl [18] and aluminium in weak alkaline solution [19]. To our knowledge, there has been no report concerning the corrosion behaviour of Al in sulphuric acid solution using polyacrylic acid as an inhibitor and effect of halide ion additives.

The present study was therefore undertaken to assess the corrosion behaviour of aluminium in 0.5 M H_2SO4 using polyacrylic acid as an inhibitor and also the effect of iodide ion additives on the inhibition efficiency of PAA using electrochemical methods. Electrochemical techniques are well suited for monitoring in situ any perturbation by an inhibitor with respect to electrochemical processes in the metal/corrodent interface as well as providing information on the corrosion rate. Morphological changes on the corroding Al surface has been visualised by atomic force microscopy (AFM).

Experimental

Pure cast aluminium (99.99%) used in this study was machined into test coupons of dimension 1 × 1 × 0.5 cm. The coupons were embedded in PTFE rods by epoxy resin with an exposed area of 1 cm^2. The coupons were mechanically polished with silicon abrasive paper from #400 to #1000, degreased with absolute ethanol, rinsed in distilled water and dried in warm air. A 0.5 M H_2SO_4 solution was prepared from analytical reagent grade 98% sulphuric acid using distilled water and served as the corrodent. PAA (M_n=5,000 g mol^{-1}, SCRC, China) with chemical structure of repeat unit shown below was dissolved in 0.5 M H_2SO_4 solution to obtain the desired concentration (1×10^{-5}–1×10^{-3} M) as the test inhibitor.

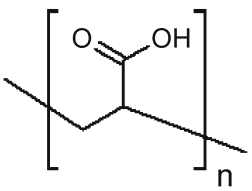

Chemical structure of PAA repeat unit

Electrochemical measurements were performed using a PARC Parstat-2273 Advanced Electrochemical System operated with Powersine and Powercorr software. A conventional electrode glass cell of 400 mL capacity was used for the experiments. Aluminium coupons were used as the working electrode, saturated calomel electrode (SCE) as reference electrode and platinum foil used as counter electrode. The SCE was connected via Luggin's capillary. Corrosion tests were carried out in the blank corrodent in the absence and presence of different concentrations of the test inhibitor (PAA). The synergistic effect of iodide ions was investigated by adding 0.5–5 mM KI into the inhibited solutions containing 1×10^{-3} M PAA. All experiments were carried out in stagnant aerated solutions at 30±1 °C. Prior to each experiment, the working electrode was immersed in the different test solutions for 30 min until a stable open circuit potential was attained. Electrochemical impedance spectroscopy (EIS) tests were made at corrosion potential (E_{corr}) over a frequency range of 100 kHz–10 mHz, with a signal amplitude perturbation of 5 mV. Spectral analyses were performed using Zsimpwin software also supplied by PARC. Potentiodynamic polarisation studies were carried out at potential range of ±250 mV with respect to the corrosion potential (E_{corr}) at a sweep rate of 0.333 mV/s. The linear Tafel segments of the anodic and cathodic curves were extrapolated to corrosion potential to obtain the corrosion current densities (i_{corr}).

Fourier transform infrared (FTIR) spectra (KBr pellet) were recorded using Nicolet-Magna-IR 560 FTIR spectrophotometer. The spectra of the protecting films in PAA (1×10^{-3} M) and PAA+5 mM KI were recorded by carefully removing the film, mixing it with KBr and making the pellet.

For AFM analyses, pure cast aluminium electrodes cut into dimensions 1 × 1 × 0.5 cm were abraded with different grades of silicon carbide abrasive paper and thereafter polished to mirror finished surfaces with diamond paste, rinsed in distilled water and then absolute ethanol and dried in warm air .They were immersed in the blank solution (0.5 M H_2SO_4) and in 1×10^{-3} M PAA and 1×10^{-3} M PAA + 5 mM KI solutions for 10 h at 30±1 °C and then washed with distilled water and dried in warm air. The exposed aluminium specimens were subjected to AFM analysis using PicoPlus scanning probe microscope, Molecular Imaging Corp.

Results and discussion

Inhibition by polyacrylic acid

The effect of polyacrylic acid of varying concentrations on the impedance behaviour of pure cast aluminium was studied at the open circuit potential at 30 °C. The Nyquist

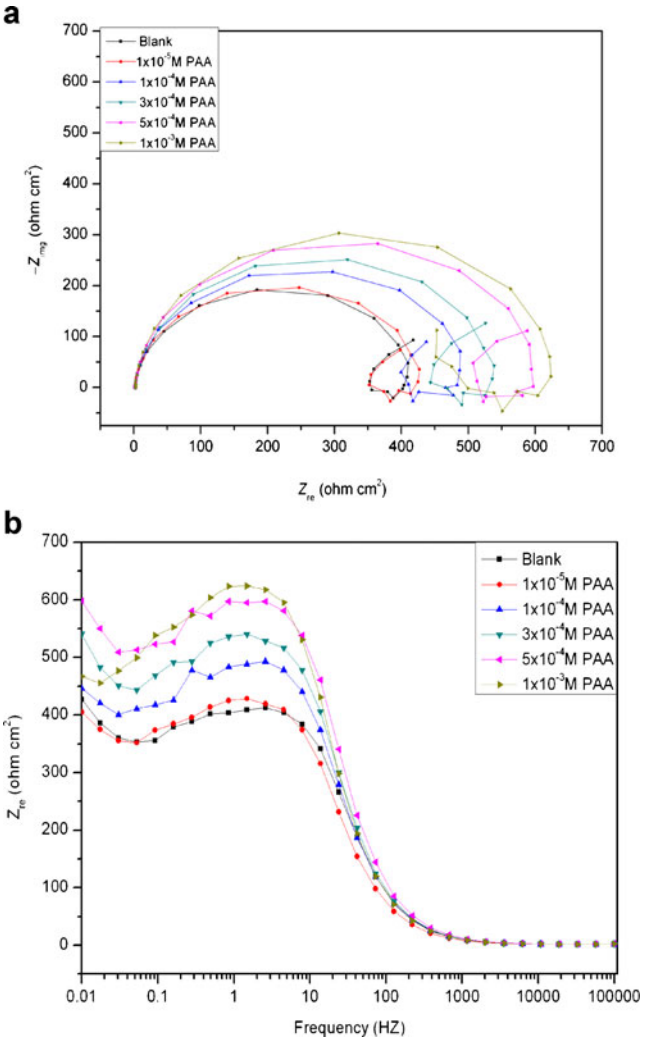

Fig. 1 Electrochemical impedance plots of Al in 0.5 M H_2SO_4 in the absence and presence of PAA: Nyquist (**a**) and Bode (**b**)

and Bode plots are depicted in Fig. 1a, and b respectively. The shape of the impedance plots for aluminium in the absence of the inhibitors is the same as reported in the literature in acid [20–22], alkaline and other media [19, 23–26]. It is observed that the shape of the impedance diagrams increases but not altered on addition of the inhibitor (PAA), suggesting that similar mechanisms for the metal dissolution in 0.5 M H_2SO_4 in the absence and presence of the inhibitor occurred. Inspection of the figure also revealed that an increase in the concentration of PAA results in an increase in the size of the semicircle and impedance of the interface in Fig. 1a, b, respectively, which is an indication of the inhibition of the corrosion process. The Nquist plots presented in Fig. 1a are characterised by three time constants consisting a large capacitive loop at high frequencies, an inductive loop at medium frequencies (MF), followed by the second capacitive loop at low frequencies (LF). There has been no general agreement in the literature regarding the origin of time constants found in the impedance diagram. The high-frequency capacitive loop could be attributed to the relaxation process in the aluminium oxide (or hydrated oxide) film present on the aluminium surface and its dielectric properties [19, 27, 28] since the oxide film is considered to be a parallel circuit of a resistor due to the ionic conduction of the oxide film and a capacitor due to its dielectric properties [28]. Another possible explanation for the origin of the capacitive loop at high frequency as put forward by Brett [29] and reported in [20] is the reactions involved in the formation of the oxide layer. Brett suggested that at the metal/oxide interface aluminium is oxidised to Al^+ intermediates. The Al^+ intermediates will subsequently be oxidised to Al^{3+} at the oxide/solution interface where also O^{2-} or OH^- is formed. At the same time with the formation of O^{2-} ions, H^+ ions are formed. This results in a local acidification at the oxide/electrolyte interface. The electrode impedance in this case was determined by the metal/oxide interface, the oxide film and the oxide/solution interface [19]. The inductive loop observed at MF may be attributed to bulk or surface relaxation of species in the oxide [30]. Adsorption of intermediates (H^+ and SO_4^{2-} ions) could also cause an inductive loop. The second capacitive loop observed at LF could be assigned to the metal dissolution [19]. An equivalent circuit of seven elements depicted in Fig. 2 was used to analyse the impedance spectra of pure cast aluminium in 0.5 M H_2SO_4 in the absence and presence of 1×10^{-3} M PAA. The model includes the solution resistance, R_s, a series combination of a film resistance R_f inductance L in parallel with inductance resistance R_L, double-layer capacitance C_{dl} in parallel with charge transfer resistance R_{ct} and the constant phase element CPE. The Nyquist plot of the impedance is a semicircle characteristics of the parallel arrangement of the double-layer capacitance and charge transfer resistance corresponding to Al–Al^+ reaction. Contribution to the total impedance at the middle frequencies comes mainly from the inductive elements. The inductor which arises from adsorption effects could be defined as (L=Rτ), where τ is the relaxation time for

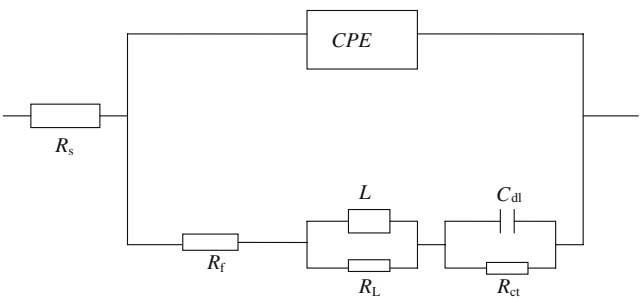

Fig. 2 Electrochemical equivalent circuit used for the simulation of impedance spectra

adsorption on the electrode surface. The circuit in the low-frequency domain includes double-layer capacitance (C_{dl}) and charge transfer resistance (R_{ct}) elements. The R_{ct} value is a measure of charge transfer resistance corresponding to the Al^{+}–Al^{3+} reaction [25].

CPE is used in this model to compensate for non-homogeneity in the system and is defined by the values of Y_o and n. The impedance is represented by

$$Z_{CPE} = Y_o^{-1}(jw)^{-n} \quad (1)$$

where Y_o is the CPE constant, n is the CPE exponent which can be used as a gauge of the heterogeneity or roughness of the surface, $j=(-1)^{1/2}$, ω is the angular frequency in rad s^{-1}, $\omega=2\ \pi f$ and f is the frequency in Hertz. If $n=1$, the impedance of CPE is identical to that of a capacitor, $Z_{CPE}=(j\omega C)^{-n}$, and in this case, Y_o gives a pure capacitance (C).

Figure 3 shows simulated and experimentally generated impedance diagrams for pure cast aluminium in 0.5 M H_2SO_4 in the absence and presence of test solutions. Excellent fit with this model was obtained for all experimental data. In this model, polarisation resistance can be calculated from Eq. 2:

$$R_p = R_f + R_L + R_{ct}. \quad (2)$$

Table 1 shows the impedance parameters recorded for pure cast aluminium in 0.5 M H_2SO_4 solution in the absence and presence of different concentrations of PAA at 30±1 °C. The data indicate that polarisation resistance increases with an increase in PAA concentration. Inspection of the table also reveals that the charge transfer resistance, R_{ct}, and double-layer resistance, C_{dl}, vary in inverse proportion at the whole concentration range. The increase in charge transfer resistance with concentration of PAA indicates that the inhibition efficiency of these molecules increase as their concentration increases. The inhibition efficiency from the impedance measurements was calculated using the relationship:

$$IE(\%) = \frac{R_{ct} - R_{ct}^{o}}{R_{ct}} \times 100 \quad (3)$$

where R_{ct}^{o} and R_{ct} are the charge transfer resistances in the absence and presence of inhibitor (PAA), respectively. The decrease in double-layer capacitance with an increase in PAA concentration may be attributed to the formation of a protective layer on the electrode surface [20, 31]. The thickness of this protective layer increases with an increase in inhibitor concentration since more inhibitor molecules are adsorbed on the electrode surface, resulting in a noticeable decrease in C_{dl}. This trend is in accordance with Helmholtz model, given by Eq. 4 [32].

$$C_{dl} = \frac{\varepsilon\varepsilon_0 A}{d} \quad (4)$$

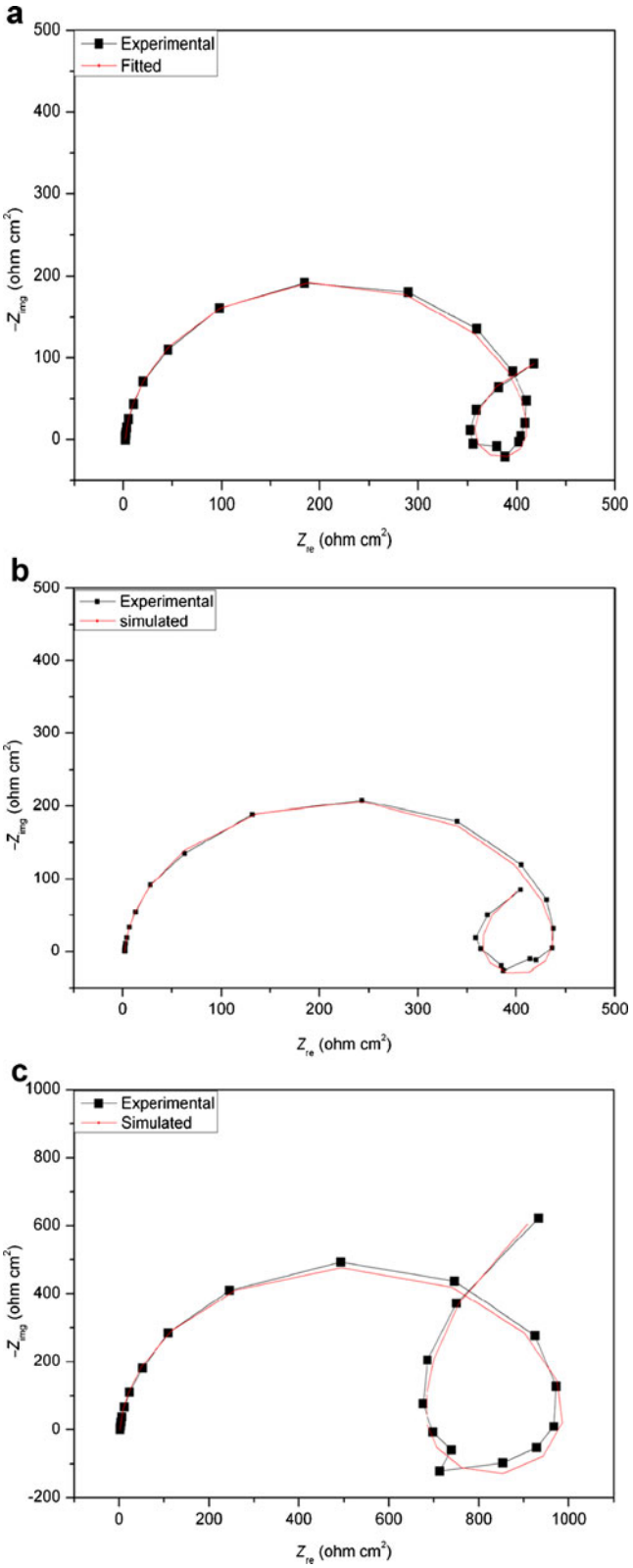

Fig. 3 Simulated and experimentally generated impedance diagrams for pure cast Al in 0.5 M H_2SO_4: **a** without inhibitor; **b** with PAA (1×10^{-3} M); and **c** with PAA+5 mM KI

Table 1 Electrochemical impedance parameters for pure aluminium in 0.5 M H_2SO_4 solution in the absence and presence of PAA

PAA concentration (M)	R_s (Ωcm^2)	Y_o ($\mu\Omega^{-1}s^n cm^{-2}$)	n	R_f (Ωcm^2)	L (Hcm^2)	R_L (Ωcm^2)	R_{ct} (Ωcm^2)	C_{dl} ($mFcm^{-2}$)	R_p (Ωcm^2)	IE%
Blank	2.03	23	0.96	423	75	90	453	118	966	–
1×10^{-5}	2.11	21	0.96	495	88	147	674	98	1316	33
1×10^{-4}	2.16	21	0.96	582	84	165	696	94	1343	35
3×10^{-4}	2.13	19	0.96	536	103	184	815	91	1535	44
5×10^{-4}	2.15	20	0.96	529	82	177	977	85	1677	54
1×10^{-3}	2.04	22	0.96	510	106	183	1087	79	1780	58

where d is the thickness of the protective layer, ε is the dielectric constant of the medium, ε_0 is the vacuum permittivity and A is the effective surface area of the electrode.

Typical polarisation curves of aluminium in 0.5 M H_2SO_4 solutions without and with different concentrations of PAA are shown in Fig. 4. It is clear from the plot that PAA affects both the cathodic and anodic part of the curves. This indicates that the inhibitor influences the dissolution of aluminium and the hydrogen evolution processes, implying that PAA functioned as a mixed-type inhibitor. It is also observed that there is no appreciable shift in the corrosion potential (E_{corr}) in the presence of different concentrations of PAA, showing that PAA afforded the inhibition of aluminium corrosion by simply blocking the available surface for both anodic and cathodic processes. In other words, the inhibitors decrease the surface area for corrosion without affecting the mechanism of corrosion and only cause inactivation of a part of the surface with respect to the corrosive medium [33]. It is also worthy of note that regarding the anodic part of the potentiodynamic polarisation curves, there is no evidence of passive film formation on the electrode surface either in the presence or absence of the inhibitor.

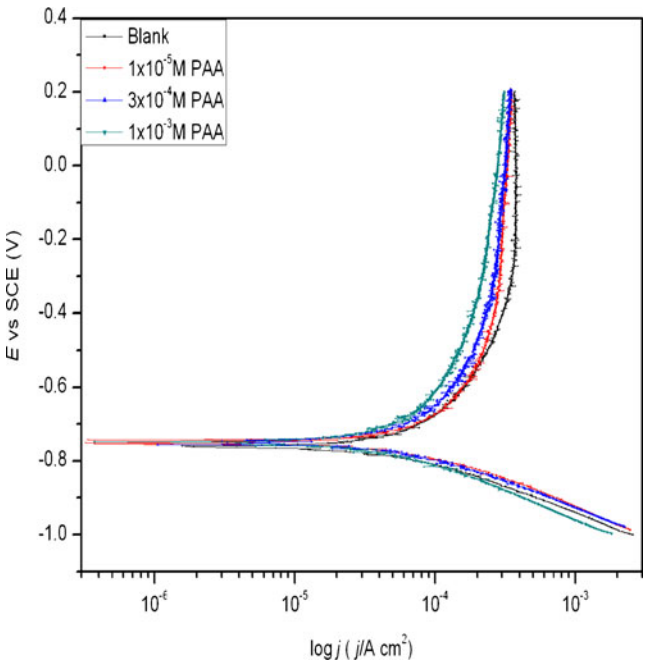

Fig. 4 Polarisation curves for Al in 0.5 M H_2SO_4 in the absence and presence of different concentrations of PAA

The electrochemical polarisation parameters for aluminium in 0.5 M H_2SO_4 solution without and containing different concentrations of PAA are listed in Table 2. The parameters include corrosion potential, E_{corr}, corrosion current densities, i_{corr}, anodic and cathodic Tafel constants as well as the inhibition efficiency (IE%). The inhibition efficiency was calculated using the relationship:

$$\mathrm{IE\%} = \left(1 - \frac{i_{corr}}{i^{o}_{corr}}\right) \times 100 \qquad (5)$$

where i^{o}_{corr} and i_{corr} are the corrosion current densities in the absence and presence of inhibitor, respectively. It is clear from the table that introduction of PAA to the acid solution causes a shift in E_{corr} to the more positive values, however with no appreciable shift in E_{corr} with increasing PAA concentration. Increasing PAA concentrations markedly reduced the corrosion current density (i_{corr}) and consequently increases inhibition efficiency. Both anodic and cathodic Tafel slopes were reduced in the presence of PAA, indicating that the inhibitor affects both anodic and cathodic corrosion reactions, hence acting as a mixed-type inhibitor. The values of inhibition efficiency are low compared to the ones obtained by EIS measurements, although they follow the same trend. The lower values of IE% from polarisation technique according to Oguzie et al. [34] could be attributed to the predominant influence of the anodic dissolution process in determining the corrosion rate.

Adsorption consideration

The metal surface in aqueous solution is always covered with adsorbed water molecules. Therefore, the adsorption of inhibitor molecules from aqueous solution is a quasi-substitution process [35, 36]. For organic inhibitors that

Table 2 Potentiodynamic polarisation parameters for pure aluminium in 0.5 M H_2SO_4 solution in the absence and presence of PAA

PAA concentration (M)	E_{corr} (mV/SCE)	i_{corr} (μAcm^{-2})	β_c (mVdec^{-1})	β_a (mVdec^{-1})	IE%
Blank	−767	165	122	334	–
1×10^{-5}	−755	133	135	529	19
1×10^{-4}	−755	116	152	551	29
3×10^{-4}	−747	112	119	407	32
5×10^{-4}	−746	101	145	558	38
1×10^{-3}	−747	100	144	473	39

have the ability to adsorb strongly on metal surface, thus hindering the dissolution reaction, the surface coverage (θ) can be evaluated as the inhibition efficiency. The relationship between inhibition efficiency and the bulk concentration of the inhibitor at constant temperature, which is known as isotherm [36], gives an insight into the adsorption process. Several adsorption isotherms were attempted to fit surface coverage values to classical isotherms of Langmuir, Temkin, Frumkin, El-Awady et al. and Freundlich [37] as well as substitutional isotherms of Flory–Huggins, Dhar–Flory–Huggins and Bockris–Swinkles [38]. The value of correlation coefficient (R^2) was used to determine the best fit isotherm which was obtained for Langmuir and Frumkin isotherms. The degree of surface coverage values for various concentrations of PAA was evaluated from EIS measurements using the relationship $IE(\%) = 100 \times \theta$, assuming that the inhibitor efficiency is due mainly to the blocking effect of the adsorbed species [37, 39, 40]. Figure 5 shows a typical Langmuir isotherm obtained by plotting C/θ as a function of C (inhibitor concentration). A linear plot was obtained with a correlation coefficient of 0.995 and slope of 1.655. A Langmuir isotherm assumes that the solid surface contains a fixed number of adsorption sites and each site holds one adsorbed species [41]. Langmuir isotherm can be represented by the relation:

$$\frac{C}{\theta} = \frac{1}{K_{ads}} + C \tag{6}$$

where C is the inhibitor concentration, θ is the degree of surface coverage and K_{ads} is the equilibrium constant of adsorption process. Though the linearity of the plot and good correlation coefficient may be interpreted to suggest that the experimental data for the inhibitor obeys the Langmuir adsorption isotherm, considerable deviation of the slope from unity shows that the isotherm may not be strictly applied. This deviation from unity is attributable to interactions between the adsorbed species on the metal surface.

The Frumkin isotherm is commonly used to quantify the interactions occurring between corrosion inhibitor and a metal surface [37, 42–44], and it is expressed by the relationship [42]:

$$\left(\frac{\theta}{1-\theta}\right)\exp(-f\theta) = c\left[\frac{1}{55.5}\exp\left(\frac{-\Delta G^{o}_{ads}}{RT}\right)\right] \tag{7}$$

where θ is the degree of surface coverage, f is the interaction term parameter ($f>0$ for lateral attraction between adsorbed PAA molecules and $f<0$ for lateral repulsions between PAA molecules), c is the concentration of inhibitor, 55.5 is the concentration of water in solution (in mol dm^{-3}), ΔG^{o}_{ads} is the standard free energy of adsorption (kJ mol^{-1}), R is the gas constant and T is the absolute temperature. The Frumkin adsorption isotherm is a general expression since the limiting case for which $f=0$ is representative of an interaction free behaviour between adsorbed species and defined the Langmuir isotherm [37, 42]. Because the logarithmic term is very sensitive to inaccuracy in determining θ values at the limiting values of the surface coverage [42], two values of θ in the range 0.3–0.6 and their corresponding PAA concentration were selected for the computation of f and ΔG^{o}_{ads} parameters according to Eq. 7 [41, 42]. From the values of f and ΔG^{o}_{ads} determined, Eq. 7 can be rearranged to give [42]:

$$\log c = \log\left(\frac{\theta}{1-\theta}\right) + A\theta + B \tag{8}$$

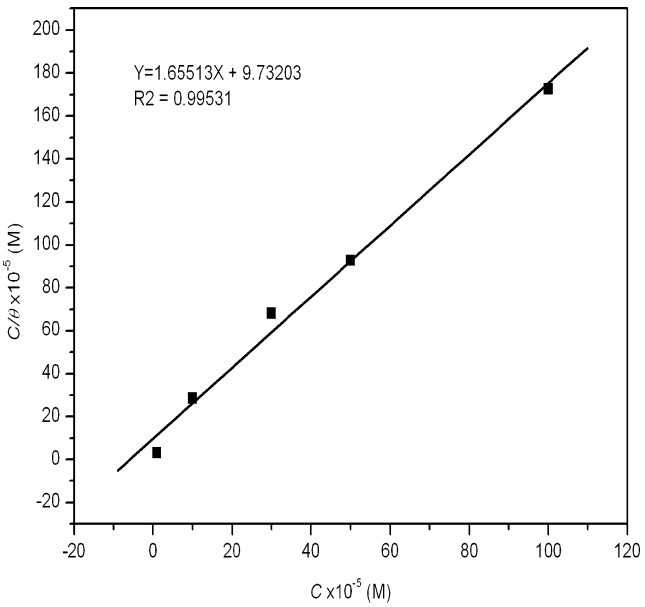

Fig. 5 Langmuir adsorption isotherm for PAA on pure cast alumium in 0.5 M H_2SO_4 at 30 °C

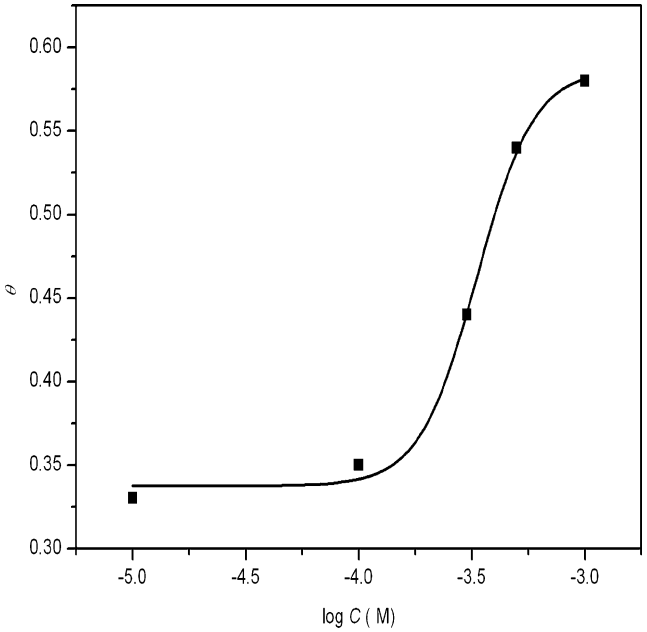

Fig. 6 Frumkin adsorption isotherm for PAA on pure cast aluminium in 0.5 M H_2SO_4 at 30 °C

where $A=-f/2.303$ and $B = \left(\Delta G^{o}_{ads}/2.303RT\right) + \log 55.5$ and has the meaning of equilibrium constant of the adsorption process. Equation 8 was used to plot the Frumkin isotherm depicted in Fig. 6 as θ against log C. S-shaped curve was obtained, which is consistent with the Frumkin adsorption isotherm. The existence of adsorption interactions between adsorbed PAA molecules is thus confirmed since most of the experimental data fit nicely into the Frumkin isotherm plots. The adsorption parameters B, f and ΔG^{o}_{ads} obtained were 1.75 M^{-1}, −7.5 and −22.97 kJ/mol, respectively. The negative value of ΔG^{o}_{ads} indicates spontaneous adsorption of PAA molecules onto the aluminium surface. Values of ΔG^{o}_{ads} around −20 kJ/mol or lower are consistent with the electrostatic interaction between charged organic molecules and charge metal surface (physisorption), whilst those around −40 kJ/mol or higher involve charge sharing or transfer from the inhibitor molecules to the metal surface to form a coordinate type of bond (chemisorption) [36]. The value of ΔG^{o}_{ads} obtained in this study is below −40 kJ/mol, which therefore indicates that PAA molecules were physically adsorbed onto the aluminium surface. The negative value of f indicates that the adsorption of the tested compound is accompanied by mutual repulsion of the molecules [45].

Effect of iodide ions

As a result of low inhibition efficiency obtained for PAA alone, studies involving the addition of various concentrations of iodide ions to PAA were undertaken. It has been reported that combination of some organic inhibitors with halide ions yield useful enhancement in inhibition efficiency due to synergistic action between the halide ions and the organic inhibitor [45–47]. Figure 7 shows the impedance diagram for aluminium in 0.5 M H_2SO_4 solutions containing different concentrations of iodide ions. The curves are similar to the one obtained for the blank solution and are characterised by three time constants. However, the size of the diameter of the semicircle in the Nyquist plot increased in the presence of the iodide ions compared to the blank and increases with an increase in the concentration of iodide ions, showing that the iodide ion was adsorbed onto the aluminium surface replacing the water molecules and/or other species present on the metal surface. A similar observation has been reported in the literature [48]. The inhibition efficiency obtained on addition of 0.5, 1, 2.5 and 5 mM KI were 51%, 56%, 66% and 67%, respectively.

Figure 8a, b shows the impedance behaviour of pure cast aluminium in 0.5 M H_2SO_4 containing 1×10^{-3} M PAA in combination with 0.5–5 mM KI corresponding to Nyquist and Bode, plots respectively. Inspection of the figures shows that the diameters of the semicircles in Nyquist plot and the impedance of the interface in Bode plot increases with an increase in the concentration of KI. It is also observed that the addition of iodide ions increases the impedance but does not change other aspects of the behaviour. Again, these results indicate that almost no change in the corrosion mechanism occurred due to iodide ions addition. The impedance data were analysed using the equivalent circuit shown in Fig. 2, and the corresponding electrochemical parameters are given in Table 3. It is clear from the table that the addition of iodide ions to 1×10^{-3} M PAA increased the polarisation resistance (R_p), charge transfer resistance (R_{ct}) and decreased double-layer capac-

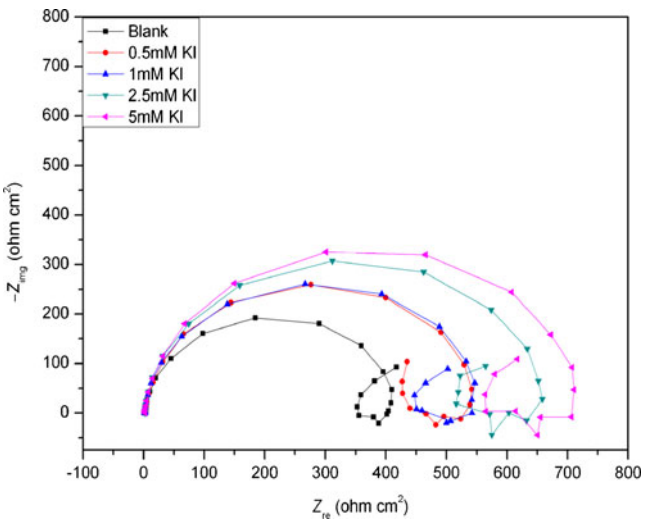

Fig. 7 Electrochemical impedance plots of Al in 0.5 M H_2SO_4 in the absence and presence of different concentrations of KI

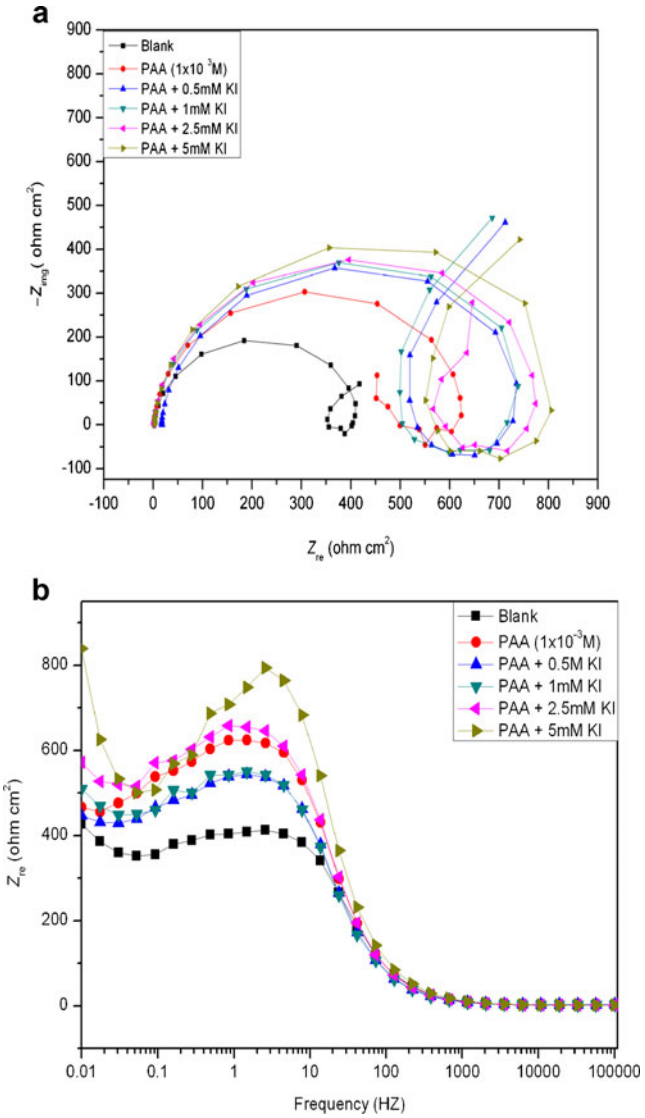

Fig. 8 Electrochemical impedance plots of Al in 0.5 M H_2SO_4 in the absence and presence of 1×10^{-3} M PAA in combination with different concentrations of KI: Nyquist (**a**) and Bode (**b**)

itance (C_{dl}). Polarisation resistance was increased from 1,780 to 2,271–2,459 Ω cm^2 for 0.5–5 mM KI concentration, whilst charge transfer resistance was increased from 1,087 to 1,370–1,619 Ω cm^2 in the same KI concentration range. Also, the double-layer capacitance (C_{dl}) decreased from 79 mF cm^{-2} for 1×10^{-3} M PAA to 29, 27, 24 and 24 mF cm^{-2} on addition of 0.5, 1, 2.5 and 5 mM KI, respectively, to 1×10^{-3} M PAA. Inhibition efficiency increases from 58% in the presence of 1×10^{-3} M PAA to 67–72% on addition of different concentrations of KI (0.5–5 mM) to 1×10^{-3} M PAA solution. The improved inhibition efficiency caused by the addition of iodide ions to PAA is due to synergistic effect.

The effect of the addition of iodide ions on the corrosion inhibition performance of polyacrylic acid for pure cast aluminium in 0.5 M H_2SO_4 was also studied using potentiodynamic polarisation measurements. Before studies involving iodide ions–PAA mixtures, polarisation behaviour of aluminium in the presence of different concentration of iodide ions was undertaken. The polarisation curves (not shown) revealed that the corrosion potential shifted negatively and both anodic and cathodic current densities were affected. A similar observation has been reported for Br^- ion by Tang et al. [49] in their study of synergistic inhibition between hexadecyl trimethyl ammonium bromide and NaBr for corrosion of cold rolled steel in 0.5 M H_2SO_4. The shift in E_{corr} to less noble values in the presence of halide ions was interpreted to mean that the corrosion reaction was under cathodic control. The inhibition efficiency obtained for the different concentrations of iodide ions, 0.5, 1, 2.5 and 5 mM KI, from polarisation measurements were 47%, 56%, 63% and 64%, respectively.

Figure 9 shows the anodic and cathodic polarisation behaviour of Al in 0.5 M H_2SO_4 containing PAA (1×10^{-3} M) and PAA in combination with varying concentrations of iodide ions. The figure clearly shows that the addition of iodide ions to PAA slightly shifts the corrosion potential to a more negative direction. Further inspection of Fig. 9 showed that on introduction of KI to PAA, a plateau in the current was observed around the region of potential higher than −0.3 V, indicating passivation in the surface for 1 mM KI concentration. At concentrations above 1 mM KI, an abrupt increase in current is seen at potentials around 0.1 V, indicating a break in the passive film formed on the Al surface. The observed passivation may be considered as

Table 3 Electrochemical impedance parameters for pure aluminium in 0.5 M H_2SO_4 solution containing 1×10^{-3} M PAA and PAA + KI mixtures at 30 °C

System/concentration	R_s (Ωcm^2)	Y_o (μΩ^{-1}s^{n}cm^{-2})	n	R_f (Ωcm^2)	L (Hcm^2)	R_L (Ωcm^2)	R_{ct} (Ωcm^2)	C_{dl} (mFcm^{-2})	R_p (Ωcm^2)	IE%
Blank	2.03	23	0.96	423	75	90	453	118	966	–
PAA (1×10^{-3} M)	2.04	22	0.96	510	106	183	1,087	79	1,780	58
PAA+0.5 mM KI	2.16	18	0.95	595	113	306	1,370	29	2,271	67
PAA+1 mM KI	2.11	17	0.96	551	100	281	1,546	27	2,379	71
PAA+2.5 mM KI	2.19	19	0.96	553	101	266	1,601	24	2,419	72
PAA+5 mM KI	2.08	18	0.96	566	94	275	1,619	24	2,459	72

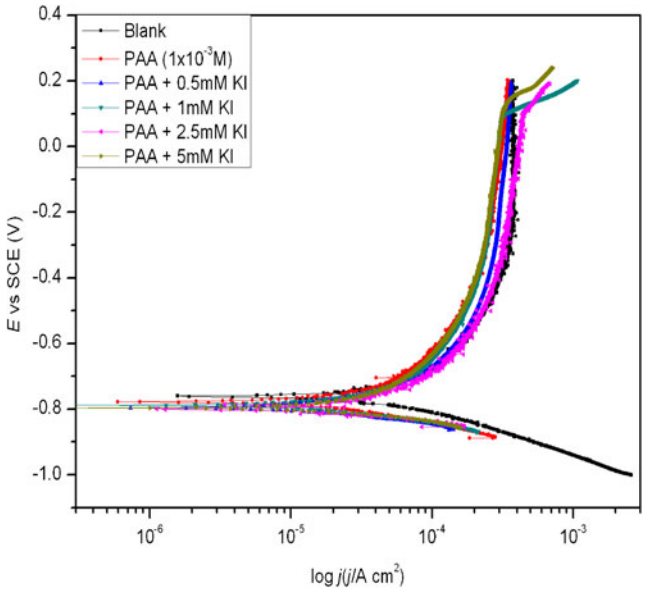

Fig. 9 Polarisation curves for Al in 0.5 M H_2SO_4 in the absence and presence of 1×10^{-3} M PAA in combination with different concentrations of KI

an improvement of the inhibition effect of PAA on addition of KI. Table 4 lists the electrochemical parameters associated with polarisation measurements recorded for pure cast Al in 0.5 M H_2SO_4 solution in the absence and presence PAA alone and in combination of different concentrations of iodide ions. It is obvious that comparing the data of PAA alone and that of PAA + KI mixtures, the corrosion current densities and hence rate of corrosion of PAA are significantly decreased upon the introduction of iodide ions to PAA/H_2SO_4-containing solutions. The decrease in corrosion current densities enhances with an increase in the concentration of iodide ions. It is also very clear from the data presented in the table that the addition of iodide ions to PAA–H_2SO_4 solutions results in a marked decrease in both anodic and cathodic current densities. A shift in E_{corr} towards more negative potential was also observed here. Both the anodic and cathodic Tafel slopes were also affected on introduction of iodide ions into PAA-containing solutions. This indicates that PAA in the presence of I^- ions is an effective mixed-type inhibitor for Al corrosion in sulphuric acid solution. Amin et al. [50] and Zhang et al. [51] have reported similar observations in their investigations of synergistic effect of I^- ions on the corrosion inhibition of Al in 1.0 M phosphoric acid solutions by purine and arginine self-assembled monolayers against copper corrosion in 0.5 M HCl, respectively. The values of inhibition efficiency computed using Eq. 5 are also listed in Table 4. Inhibition efficiency of PAA (1×10^{-3} M) increased in the presence of iodide ions from 39% to the range 74–87%. This result indicates the existence of a strong synergism between PAA and iodide ions in the inhibition of Al in these solutions. The results obtained for EIS and polarisation techniques for PAA–KI combination is in good agreement.

The existence of synergism phenomenon between PAA and iodide ions was further evaluated by estimating the synergism parameter, S_1, from the inhibition efficiency values from the two techniques employed according to Aramaki and Hackermann and reported elsewhere [44, 52, 53] as follows:

$$S_1 = \frac{1 - I_{1+2}}{1 - I'_{1+2}} \tag{9}$$

where $I_{1+2} = I_1 + I_2$, I_1 the is inhibition efficiency of the iodide ions, I_2 is the inhibition efficiency of polyacrylic acid and I'_{1+2} is the measured inhibition efficiency for the polyacrylic acid in combination with the iodide ions. The estimated values of S_1 are listed in Table 5. The computed values of the synergistic parameter shown in the table for the different concentrations of iodide ions are greater than unity. This demonstrates that the enhanced inhibition efficiency of PAA caused by the addition of iodide ions is due mainly to synergistic effect. The observed synergistic effect between PAA and iodide ions may be explained as follows: In acid medium, PAA may be protonated, thus becoming a cation existing in equilibrium with the corresponding molecular form. It is also well known that terminal oxygen atoms at metal oxide surfaces react with water, forming hydroxylated sites or hydroxide layers at the surface (M–OH) that impart a pH-dependent surface charge. An oxide or hydroxide surface (M–OH)

Table 4 Potentiodynamic polarisation parameters for pure aluminium in 0.5 M H_2SO_4 solution containing 1×10^{-3} M PAA and PAA + KI mixtures at 30 °C

System/concentration	E_{corr} (mV/SCE)	i_{corr} (μAcm^{-2})	β_c (mVdec^{-1})	β_a (mVdec^{-1})	*IE%*
Blank	−767	165	122	334	–
PAA (1×10^{-3})	−747	100	144	473	39
PAA+0.5 mM KI	−795	43	117	443	74
PAA+1 mM KI	−791	41	109	513	75
PAA+2.5 mM KI	−796	35	84	426	79
PAA+5 mM KI	−800	20	61	179	87

Table 5 Synergistic parameter (S_1) for the different concentration of KI from EIS and potentiodynamic polarisation methods at 30 °C

KI concentration (mM)	Synergism parameter (S_1)	
	EIS method	Potentiodynamic polarisation method
0.5	1.64	1.17
1	1.61	1.26
2.5	1.75	1.29
5	1.75	1.19

becomes charged by reacting with H^+ or OH^- ions due to surface amphoteric reactions Eqs. 10 and 11. At low pH, hydroxide surface adsorbs protons to produce positively charged surfaces ($M–OH_2^+$), and at high pH, they lose protons to produce negatively charged surfaces ($M–O^-$) [50]:

$$M - OH + H^+ \quad \rightleftarrows \quad M - OH_2{}^+ \tag{10}$$

$$M - OH + OH^- \quad \rightleftarrows \quad M - O^- + H_2O. \tag{11}$$

The number of these sites and the surface charge of the oxide are determined by the pH of the solution. Surface charge influences the adsorption of ions from solution and other interfacial phenomenon [54]. The pH of potential zero charge for aluminium oxides/hydroxides is between 6 and 9, and in acidic solution, the accumulation of $Al–OH_2^+$ species accounts for the surface charge [50, 55, 56].

In acidic solution, therefore, the positively charged surface sites will elctrostatically attract any anions present in solution and repel cations. Hence, poor adsorption is expected to occur between protonated PAA molecules and the positively charged surface of Al oxide film. This may probably account for the low inhibition efficiency (39% for polarisation technique for example) recorded for only PAA molecules under these conditions. Iodide ions are usually characterised by strong adsorbability on metal surfaces. Iodide ions are first adsorbed at the oxide/solution interface at the corrosion potential through electrostactic attraction force due to the excessive positive charge at the oxide/solution interface. This process changes the charge of the solution side of the interface from positive to negative [50]. This change in the charge of the solution side at the interface facilitates physical adsorption of the inhibitor's cation. Thus, the protonated PAA molecules are able to electrostatically adsorb on the electrode surface covered with primary adsorbed iodide ions. It is obvious that iodide ions promote physical adsorption of PAA on the Al surface. The stabilisation of the adsorption of inhibitor on the Al surface caused by the interaction between protonated PAA molecules and iodide ions leads to greater surface coverage and hence greater corrosion inhibition.

FTIR spectra analysis

FTIR analysis was undertaken to assess the role vis-à-vis the possible mechanism through which the iodide ions exert their synergistic influence. Earlier studies [57] in this laboratory showed that the spectra of films extracted from iron surface in 0.1 M H_2SO_4 containing thiourea (TU) and thiourea–iodide ion mixtures were different, indicating that the interfacial species become chemically altered in the presence of iodide ions. Two mechanisms were proposed to account for the observed transformation of TU_{ads}; it was either TU was chemically transformed on the Fe surface or in solution in the TU–iodide ion medium. The former effect was not expected to modify the FTIR spectra since the interaction is likely to be purely electrostatic. It was concluded that the iodide ion reacts with TU rather than getting adsorbed on the Fe surface, resulting in the formation of new reaction products that get adsorbed on the Fe surface, and this probably was responsible for the modification of the infrared spectra in TU–iodide ion media.

Figure 10 shows the IR spectra in the region 400–4,000 cm^{-1} of films carefully removed from the aluminium surface immersed in 0.5 M H_2SO_4 solution containing 1×10^{-3} M PAA and 1×10^{-3} M PAA + 5 mM KI at 30 °C. It is seen from the figure that both spectra exhibit the same characteristic absorption bands typical of polyacrylic acid without and with iodide ions. Important absorption bands at 3,068, 1,667 and 1,095 cm^{-1} corresponding to –OH stretch, asymmetric stretching of C–O of carboxylate anion, C–O stretch and other bands typical of polyacrylic acid could be discerned from the spectra and indicated that PAA

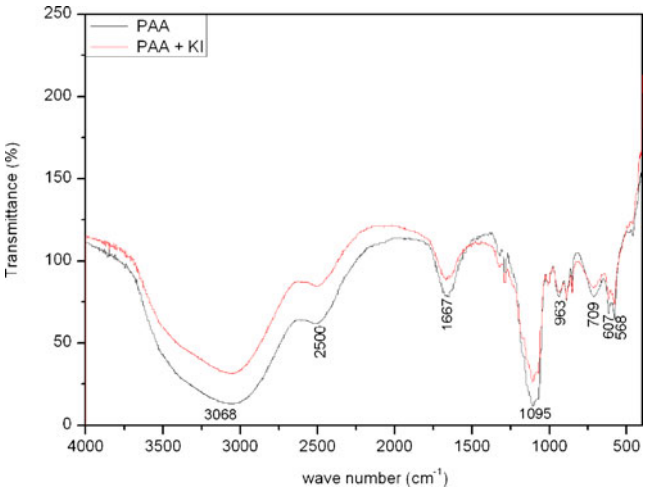

Fig. 10 FTIR spectra of film on aluminium in 0.5 M H_2SO_4 in containing 1×10^{-3} M PAA and 1×10^{-3} M PAA + 5 mM KI

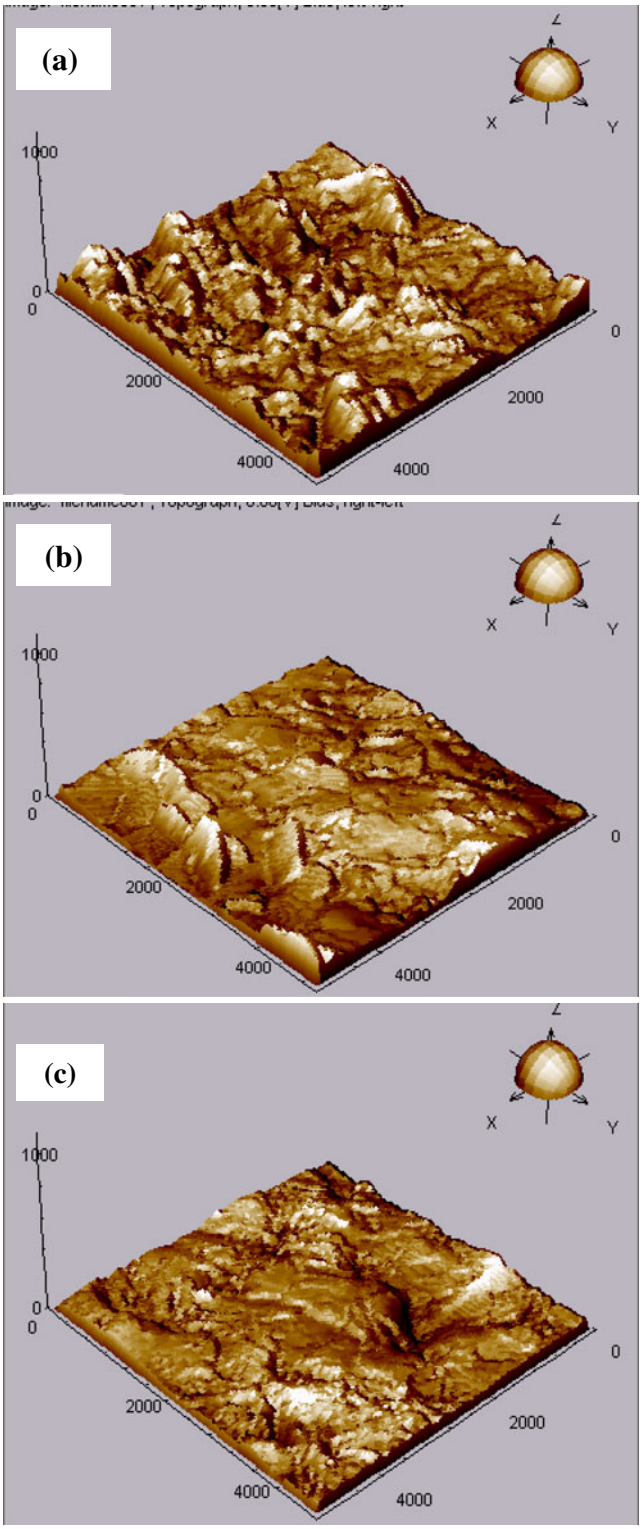

Fig. 11 AFM three-dimensional images of Al in 0.5 M H_2SO_4: **a** without inhibitor; **b** containing 1×10^{-3} M PAA; and **c** containing 1×10^{-3} M PAA + 5 mM KI. Scale: *X* = nm; *Y* = nm; *Z* = nm

molecules were adsorbed on the surface of the pure aluminium. Relating the results of the present study to the ion-pair interactions leading up to inhibitor-halide synergism, the more acceptable situation is the one in which the ion-pair formation occurs directly on the metal surface as follows:

$$I^-_s \rightarrow I^-_{ads} \quad (12)$$

$$I^-_{ads} + PAA^+ \rightarrow (I^- - PAA^+)_{ads} \quad (13)$$

where I_s^-, PAA_s^+ and $(I^- - PAA^+)_s$ represent the halide ions, inhibitor and ion-pair, respectively, in the bulk of the solution, whilst I_{ads}^-, PAA_{ads}^+ and $(I^- - PAA^+)_{ads}$ represent

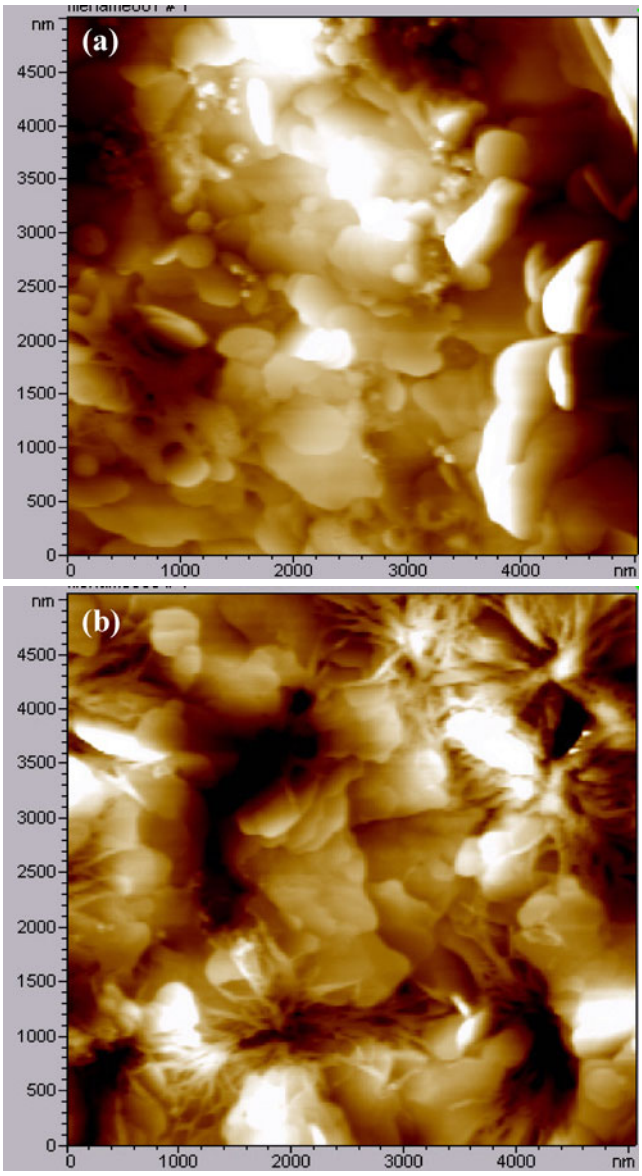

Fig. 12 AFM two-dimensional images of Al in 0.5 M H_2SO_4: containing 1×10^{-3} M PAA (**a**) and containing 1×10^{-3} M PAA + 5 mM KI (**b**). Scale: *X* = nm; *Y* = nm; *Z* = nm

the same species in the adsorbed state. This result suggests that the synergistic effect of PAA and iodide ions is cooperative in nature. The inhibitor molecule was not adsorbed directly onto the aluminium surface but by coulombic attraction to the already chemisorbed layer of the iodide ions.

Surface morphological studies

AFM is a powerful technique to characterise surface morphology at nano- to microscale and has become a new choice to study the influence of inhibitors on the generation and the progress of the corrosion at the metal/solution interface [58]. Pure aluminium specimens after immersion for 10 h in 0.5 M H_2SO_4 solution without inhibitor, with inhibitor and inhibitor–iodide ion mixtures were observed by AFM in the range 0–5,000 nm. The recorded three-dimensional images are given in Fig. 11, whilst the corresponding two-dimensional images for specimens immersed in solutions containing inhibitor and inhibitor–iodide ion mixtures are shown in Fig. 12. A rough surface is observed due to rapid corrosion of the aluminium specimen in the absence of inhibitor (Fig. 11a), resulting in protrusions and depressions of the aluminium surface. In the presence of inhibitor (PAA), the surface roughness is observed to be visibly reduced, which could be attributed to the inhibition ability of PAA. The inhibition of aluminium corrosion in 0.5 M H_2SO_4 by PAA caused by adsorption of its molecules resulted in some big spherical particles decorating the aluminium surface (Fig. 12a). The coverage, however, was not uniform as some parts of the metal were still exposed to the corrodent attack. In the presence of both PAA and iodide ions, Fig. 12b revealed that the surface of aluminium is fully and orderly covered with unique particles that are quite different and do not exist in Fig. 12a. This could be ascribed to the co-adsorption film of the mixture of PAA and KI. The inhibitor layer is observed to be much more compact and homogeneous.

Conclusions

Polyacrylic acid is found to inhibit the corrosion of pure cast aluminium in 0.5 M H_2SO_4 solution at 30±1 °C. Inhibition efficiency increases with increasing inhibitor concentration. The value of Gibbs free energy of adsorption indicates that PAA is physically adsorbed on the surface of the metal following Frumkin adsorption model. The results of potentiondynamic polarisation measurements indicate that PAA behaved as a mixed inhibitor. Inhibition efficiency of PA was enhanced by the addition of iodide ions due to synergistic effect. The synergistic effect of iodide ions and PAA is due to the co-adsorption of iodide ions and PAA molecules which is cooperative in nature.

Acknowledgements S.A Umoren acknowledges the Chinese Academy of Sciences (CAS) and Academy of Sciences for the Developing World (TWAS) for the CAS-TWAS Postdoctoral Fellowship.

References

1. Ashassi-Sorkhabi H, Shabani B, Aligholipour B, Seifzadeh D (2006) Appl Surf Sci 252:4039
2. Abd El Rehim SS, Amin MA, Moussa SO, Ellithy AS (2008) Mater Chem Phys 112:898
3. Khaled KF, Qahtani M (2009) Mater Chem Phys 113:150
4. Abdel Rehim SS, Hassan HH, Amin MA (2002) Appl Surf Sci 187:279
5. Fouda AS, Al-Sarawy AA, Ahmed FSh, El-Abbasy HM (2009) Corros Sci 51:485
6. Abdel Rehim SS, Hassan HH, Amin MA (2004) Corros Sci 46:5
7. Obot IB, Obi-Egbedi NO, Umoren SA (2009) Corros Sci 51:1868
8. Tomcsányi L, Varga K, Bartik I, Horányi H, Maleczki E (1989) Electrochim Acta 34:855
9. Øvari F, Tomcsányi L, Túrmezey T (1988) Electrochim Acta 33:323
10. Foad El-Sherbini EE, Abd-El-Wahab SM, Deyab MA (2003) Mater Chem Phys 82:631
11. Rajendran S, Sridevi SP, Anthony N, John AA, Sundearavadivelu M (2005) Anti-corros Methods Mater 52:102
12. Jianguo J, Lin W, Otieno-Alego V, Schweinsberg DP (1995) Corros Sci 37:975
13. Yurt A, Bütün V, Duran B (2007) Mater Chem Phys 105:114
14. Umoren SA, Ogbobe O, Ebenso EE, Okafor PC (2007) J Appl Polym Sci 105:3363
15. Lehr IL, Saidman SB (2006) Electrochim Acta 51:3249
16. Abdallah M, Megahed HE, El-Etre AY, Obeid MA, Mabrouk EM (2004) Bull Electrochem 20:277
17. Umoren SA, Ebenso EE (2008) Ind J Chem Technol 15:355
18. Khairou KS, El-Sayed A (2001) J Appl Polym Sci 88:866
19. Amin MA, AbdEl-Rehim SS, El-Sherbini EEF, Hazzazi OA, Abbas MN (2009) Corros Sci 51:658
20. Khaled KF, Amin MA (2009) J Appl Electrochem 39:2553
21. Brett CMA (1989) Portg Electrochim Acta 7:123
22. Lenderink HJW, Liden MVD, Wit JHWDE (1993) Electrochim Acta 38:1898
23. Abd El Rehim SS, Hassan HH, Amin MA (2002) Appl Surf Sci 187:279
24. Noor EA (2009) J Appl Electrochem 39:1465
25. Abdel-Gaber AM, Khamis E, Abo-ElDahab H, Adeel Sh (2008) Mater Chem Phys 109:297
26. Emregul KC, Aksut AA (2000) Corros Sci 42:2051
27. Mansfeld F, Lin S, Kim K, Shih H (1987) Corros Sci 27:997
28. Mansfeld F, Lin S, Kim K, Shih H (1988) Werkst Korros 39:487
29. Brett CMA (1990) J Appl Electrochem 20:1000
30. Frers SE, Stefenel MM, Mayer CM, Chierchie T (1990) J Appl Electrochem 20:996
31. Macfferty E, Hackermann N (1972) J Electrochem Soc 119:146
32. Battaillon C, Brunet S (1994) Electrochim Acta 39:455
33. Abd El Rehim SS, Hassan HH, Amin MA (2004) Corros Sci 46:5
34. Oguzie EE, Li Y, Wang FH (2007) J Solid State Electrochem 12:721
35. Chauhan LR, Gunasekaran G (2007) Corros Sci 49:1143
36. Keleş H, Keleş M, Dehri İ, Serindağ O (2008) Colloids Surf A: Physiochem Eng Aspects 320:138
37. Christov M, Popova A (2004) Corros Sci 46:1613
38. Martinez S (2002) Mater Chem Phys 77:97
39. Christov M, Popova A, Vasilev A (2007) Corros Sci 49:3276
40. Bentiss F, Traisnel M, Gengembre L, Lagrenée M (1999) Appl Surf Sci 152:237

41. Ali SA, Saeed MT, Rahman SU (2003) Corros Sci 45:253
42. Gallant D, Pézolet M, Simard S (2007) Electrochim Acta 52:4927
43. Tebbji K, Oudda H, Hammouti B, Benkaddour M, El Kodadi M, Ramdani A (2004) Colloids Surf A: Physiochem Eng Aspects 259:143
44. Oguzie EE, Onuoha GN, Onuchukwu AI (2005) Mater Chem Phys 89:305
45. Fouda AS, Mostafa HA, El-taib F, Elewady GY (2005) Corros Sci 47:198
46. Shibli SMA, Saji VS (2005) Corros Sci 47:2213
47. Mu GN, Li X, Li F (2004) Mater Chem Phys 86:59
48. Okafor PC, Zheng Y (2009) Corros Sci 51:850
49. Tang L, Li X, Mu G, Liu G, Li L, Liu H, Si Y (2006) J Mater Sci 41:3063
50. Amin MA, Mohsen Q, Hazzazi OA (2009) Mater Chem Phys 114:908
51. Zhang D, He X, Cai Q (2009) J Appl Electrochem 39:1193
52. Umoren SA, Ogbobe O, Igwe IO, Ebenso EE (2008) Corros Sci 50:1998
53. Abdel Rehim SS, Hazzazi OA, Amin MA, Khaled KF (2008) Corros Sci 50:2258
54. Brown GE (1999) Chem Rev 99:77
55. Hohl H, Stumm M (1976) J Colloid Interface Sci 55:281
56. Wood R, Fornasiero D, Ralston R (1990) Colloids Surf 51:389
57. Oguzie EE, Wang SG, Li Y, Wang FH (2009) J Phys Chem C 113:8420
58. Satapathy AK, Gunasekaran G, Sahoo SC, Amit K, Rodrigues PV (2009) Corros Sci 51:2848